MODAL COMPOSITION OF MARTIAN LOW ALBEDO REGIONS FROM OMEGA REFLECTANCE SPECTRA: IMPLICATIONS FOR UPPER CRUSTAL PETROLOGY. F. Poulet[1], B. Platevoet[2], J.-M. Bardintzeff[2], N. Mangold[2], J.-P. Bibring[1], J.F. Mustard[3], Y. Langevin[1], M. Vincendon[1], A. Aleon[1], B. Gondet[1] and P. Pinet[4], [1]Institut d'Astrophysique Spatiale, Bât. 121, Université Paris-Sud, 91405 Orsay Cedex, France, [2]IDES, Bât. 509, Université Paris-Sud, 91405 Orsay Cedex, France, [3]Department of Geological Sciences, Brown University, Providence, USA, [4]Observatoire Midi-Pyrénées, 31400 Toulouse, France. (Email: francois.poulet@ias.u-psud.fr).

Introduction: Using classical methods of spectral identification (spectral parameter, Modified Gaussian Model, linear mixing), OMEGA has provided a consensus on the identification and spatial distribution of several classes of mafic minerals [1-3]. The Noachian crust is enriched in low-Ca pyroxene, with respect to more recent lavas flows in which high-Ca pyroxene dominates, whereas olivine is present without hydrated phases in dunes and eroded layers corresponding to ancient lava flows or melt ejectas. TES data have shown that mineralogical diversity of the low albedo regions occurs at global and regional scales, including spatial variations in plagioclase, pyroxene, high-silica phases, and olivine [4-8]. [4] first identified two global end-members: 1) Surface Type 1, which occurs primarily in the southern highlands, and 2) Surface Type 2, which is found primarily in the northern lowlands. More recently, [9] found that the Martian dark regions could be classified into four groups based on relative abundances of plagioclase, pyroxene, olivine, and high-silica phase(s) (primary or secondary silicate minerals, glasses or mineraloids with Si/O ratios > 0.35).

Objective: The objective of this work is to: 1) determine the modal mineralogy of different low albedo regions using OMEGA data, 2) clarify the mineral distributions previously identified in [3], 3) compare the modal and elemental composition with those derived from TES analyses [4-10], and 4) identify possible relationship with the diverse compositions of SNCs.

Approach: One of the significant challenges for the use of reflectance spectroscopy for analyzing planetary soil mineralogy is the relationships between the band depth absorptions and mineral abundances. In order to derive the relative abundances and the grain sizes of the Martian soil from atmospherically corrected OMEGA spectra, we use the approach adopted by [11]. This approach is based on the geometrical optics approximation and is used to transform optical constants and grain sizes into a reflectance spectrum for particulate materials. [12] showed its degree of realism and of efficiency relative to other scattering models, and in particular to the Hapke model. The model has been also tested to determine the type of mixture (sand, areal or bedrock), the relative abundances and the grain sizes of components of laboratory mineral samples [13]. We apply this model to derive the relative abundances and the grain sizes of several tens of thousand spectra extracted from specific regions of Mars enriched in mafic components. For each OMEGA spectrum, the model must reproduce the shape and depth of each absorption band, the shape of the continuum as well as the absolute value of the Lambertian albedo reflectance. A single free parameter is used to adjust the continuum spectral slope so as to account for the contribution of aerosols and/or photometric effects. The spectra are fitted in the 0.99-2.5 µm wavelength range using a simplex minimization algorithm. The quality of the fit is evaluated by the value of the Root Mean Square (RMS). The regions studied here are well representative of the low albedo regions of Mars in terms of age (Noachian and Hesperian) and geomorphology (lavas, cratered terrains, dissected terrains, dunes). Small outcrops enriched in Low-Calcium Pyroxene (LCP) located in the southern hemisphere as well as some olivine-rich terrains (Nili Patera in Syrtis Major, Nili Fossae) are also derived. The set of optical constants used as end-members must be representative of materials that are under study. Because we will apply the method to low albedo regions that are dominated by basaltic materials, the minerals are a low-calcium pyroxene (pigeonite) a high-calcium pyroxene (diopside), a Fe-rich olivine (fayalite), a Mg-rich olivine (forsterite) and a dark oxide (magnetite). The optical constants were derived using the scheme described in [13] from reflectance spectra. Feldspars are spectrally featureless in the NIR, so that the spectral modelling can lead to non-unique solutions for grain size and abundances of this component. Because the observations of the Martian surface by TES have demonstrated that the plagioclase is a major component of low albedo regions, this component (here, labradorite) is included as an end-member. Note that the spectral modelling is highly nonlinear and uses radiative transfer calculations that are very time consuming. Consequently, this procedure is restricted to analysis of selected spectra and not to the entire OMEGA data set. An example of the fit procedure applied to one spectrum extracted from the Syrtis Major lavas is shown on Figure 1.

Modal mineralogy and petrological aspects: The modal mineralogy was classified by their relative abundances of plagioclase, olivine, LCP and HCP on ternary diagrams (Fig. 2). For all the studied low-albedo regions, both HCP and LCP are modeled above

the detection limits, with HCP being the dominant pyroxene. An example of derived modal mineralogy for one region is given in Table 1. The neutral components (plagioclase for OMEGA) and pyroxene abundances are consistent with those measured by TES. By contrast, notable difference between this work and the different TES analyses is the larger abundance of LCP. Region-to-region differences in modal mineralogy exist for the low-albedo olivine-free regions. The variations of LCP abundance show a compositional trend from the oldest terrains exhibiting the largest abundance (LCP-rich outcrops, Nili Fossae highlands) to the younger ones (Syrtis lavas).

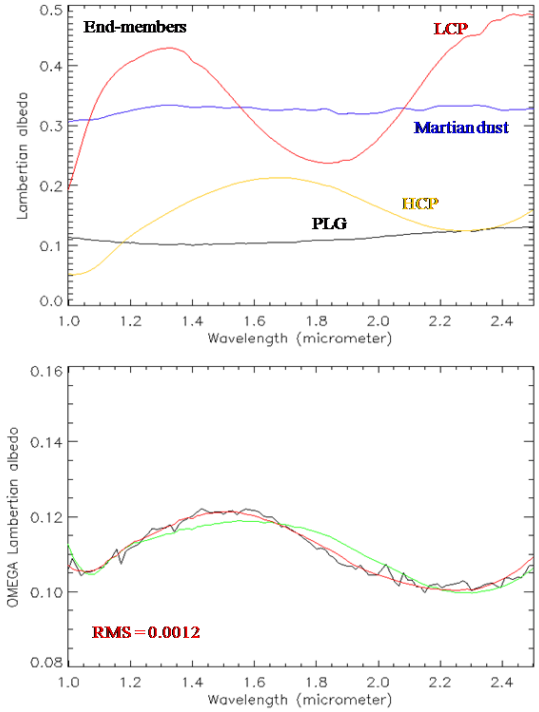

Figure 1. (**Top**) *Spectra of end-members used for the modeling of the OMEGA spectrum. (**Bottom**) The observed spectrum (solid line) is compared to two models: the best fit model (red line) and one model excluding the low-calcium pyroxene (green line).*

All calculated modal compositions are typical of gabbro-norites, except a troctolite type for the Nili Fossae area. We note a restricted distribution along the LCP/HCP side (Fig. 2), which could be related to the transition between eroded plutonic/cumulative older bedrock (enriched in LCP) to younger volcanic-type lavas. The modal mineralogy indicates an affinity with basaltic shergottites. However, the calculated plagioclase amounts (40-50 %) are equal to the maximum values found in basaltic shergottites. As it is extrapolated from the neutral component (with glass, Fe-Ti oxides,…), the plagioclase amount could be overestimated. Calculated chemical compositions of rocks, deduced from modal mineralogy and mineral compositions of the end-members, differ significantly from TES-derived compositions [10] for the Ca content. Calculated Si contents are close to those of basaltic shergottite but the ratios FeO*/MgO are lower.

Table 1. *Derived modal mineralogy for the Syrtis Major lavas and compared to the TES modal mineralogy. Values are percent and standard errors indicate +/-1σ. The neutral components correspond to plagioclase (resp. plagioclase and high-silica phases) in the case of OMEGA (resp. TES).*

	TES [9]	OMEGA [this work]
HCP	30+/-1	34+/7
LCP	4+/2	9+/-3
LCP/(HCP+LCP)	0.12+/-0.05	0.20+/-0.05
Neutral Components	46+/-6	48+/-9
Olivine (100 µm)	7+/1	<5
Others	13	8+/-5

Figure 2. *Ternary diagram to display the modal mineralogy for each studied region. The Echus lavas dated at a few hundred million years are much younger than the other regions.*

References: [1] Mustard J. F. et al. (2005) *Science, 307,* 1594-1597. [2] Bibring J-P. et al. (2006) *Science*, *312*, 400-404. [3] Poulet F. et al. (2007) *JGR, 112,* E08S02, 1-15. [4] Bandfield J. L. et al. (2000) *Science, 287,* 1626-1630. [5] Christensen P. R. et al. (2000) *JGR*, *105*, 9609-9621. [6] Christensen P. R. et al. (2001) *JGR*, *106*, 23823-23871. [7] Bandfield J. L. (2002) *JGR*, *107,* 5042. [8] Hoefen T. M. et al. (2003) *Science*, *302*, 627- 630. [9] Rogers, A. D. and P. R. Christensen (2007) *JGR, 112*, E01003.[10] McSween H. Y. et al. (2003) *JGR, 108*, 5135. [11] Shkuratov Y. et al. (1999) *Icarus, 137,* 235-246. [12] Poulet F. et al. (2002) *Icarus, 160,* 313-324. [13] Poulet F. and S. Erard (2004) *JGR, 109*, E02009.